International Journal of Biological Macromolecules 141 (2019) 313–324

Contents lists available at ScienceDirect

International Journal of Biological Macromolecules

journal homepage: http://www.elsevier.com/locate/ijbiomac

Further stabilization of lipase from *Pseudomonas fluorescens* immobilized on octyl coated nanoparticles via chemical modification with bifunctional agents

Nathalia Saraiva Rios [a,b], Eva Gomes Morais [c], Wesley dos Santos Galvão [d], Davino M. Andrade Neto [d,g], José Cleiton Sousa dos Santos [e], Felipe Bohn [f], Marcio A. Correa [g], Pierre Basílio Almeida Fechine [d], Roberto Fernandez-Lafuente [b,*], Luciana Rocha Barros Gonçalves [a,*]

[a] Departamento de Engenharia Química, Universidade Federal do Ceará, Campus do Pici, Bloco 709, 60455-760 Fortaleza, CE, Brazil
[b] Departamento de Biocatálisis, ICP-CSIC, Campus UAM-CSIC, 28049 Madrid, Spain
[c] Departamento de Bioquímica e Biologia Molecular, Universidade Federal do Ceará, Campus do Pici, Bloco 907, 60455-760 Fortaleza, CE, Brazil
[d] Departamento de Química Analítica e Físico-Química, Centro de Ciências, Universidade Federal do Ceará, Av. Mister Hull s/n, Pici, 60455-760, Fortaleza, CE CP 12200, Brazil
[e] Instituto de Engenharias e Desenvolvimento Sustentável, Universidade da Integração Internacional da Lusofonia Afro-Brasileira, Campus das Auroras, Bloco A, Rua José Franco de Oliveira, s/n, 62790790 Redenção, CE, Brazil
[f] Departamento de Física, Universidade Federal do Rio Grande do Norte, 59078-900 Natal, RN, Brazil
[g] Instituto Federal de Educação, Ciência e Tecnologia do Ceará, Campus Camocim – Rua Raimundo Cals, 2041, 62400-000 Camocim, CE, Brazil

ARTICLE INFO

Article history:
Received 8 August 2019
Received in revised form 26 August 2019
Accepted 2 September 2019
Available online 03 September 2019

Keywords:
Interfacial activation
Intermolecular crosslinking
Solid phase chemical modification
Prevention of enzyme release

ABSTRACT

The lipase from *Pseudomonas fluorescens* (PFL) was adsorbed on superparamagnetic $NiZnFe_2O_4$ octyl-nanoparticles via interfacial activation, producing the biocatalyst OCTYL-NANO-PFL. In order to further improve the stability of the immobilized lipase, the immobilized enzyme biocatalyst was chemically modified with different concentrations of diverse bifunctional molecules (glutaraldehyde (GA), divinylsulfone (DVS) or *p*-benzoquinone (BQ)). The concentrations of bifunctional agents were varied (0.5, 1, 2.5 and 5% (v/v for GA and DVS and w/v for BQ)). The results showed a greatly improved stability after chemical modification with all bifunctional molecules, mainly with 5% (v/v) GA or 1% (v/v) DVS. The biocatalysts OCTYL-NANO-PFL-GA 5% and -DVS 1% were about 60 folds more stable at pH 7 than the unmodified preparation and, at pH 5, >200 folds for 5% GA modified enzyme. The most stable BQ treated biocatalysts, OCTYL-NANO-PFL-BQ 0.5%, was about 8.3 more stable than OCTYL-NANO-PFL at pH 7, while was 20 fold more stable at pH 9.

© 2019 Elsevier B.V. All rights reserved.

1. Introduction

Lipases (E.C. 3.1.1.3) are hydrolytic enzymes with high selectivity, specificity, stability and versatility, catalyzing many different reactions, e.g. hydrolysis, esterification, interesterification, aminolysis [1–8]. Therefore, these enzymes can be used in various reactions of industrial interest for the synthesis of high value-added products [1–7,9,10]. A structural feature that is common to most lipases is the presence of a so-called "lid", composed of one [11] or even two α-helix peptides [12], that covers the active site of the lipase [13,14]. This polypeptide chain may fully isolate the lipase from the reaction medium (closed form) [3,15,16]. There some exceptions, like the lipase B from *Candida antarctica*, whose lid is small and does not isolate the active center of the lipase from the medium [17]. In the presence of hydrophobic surfaces, which can be formed by drops of hydrophobic substrates or hydrophobic solid surfaces, the open form of the lipase (where the lid moves to expose the active center) is stabilized, resulting in the so-called "open form" of the lipase [11–14]. This phenomenon may be used to immobilize, purify and stabilize lipases using hydrophobic supports, where the lipase fixes its stabilized open form via interactions between the active center surroundings and the hydrophobic support surface [18,19]. Lipase from *Pseudomonas fluorescens* (PFL) has a "true lid" [20,21]. This enzyme has many applications in biocatalysis [22,23].

Superparamagnetic nanoparticles have been used to immobilize enzymes, they are no porous supports with large surface-volume ratio, enabling a high enzyme loading [24–28]. The immobilized enzyme may be recovered by application of a magnetic field thanks to its superparamagnetism [29–34]. All the enzyme is immobilized in the external surface of the support and that prevents any internal diffusion limitations [29–37]. However, it also exposes the enzyme to external interfaces and some of the advantages regarding enzyme stabilization via immobilization inside porous supports are lost [38,39].

* Corresponding authors.
E-mail addresses: rfl@icp.csic.es (R. Fernandez-Lafuente), lrg@ufc.br (L.R.B. Gonçalves).

https://doi.org/10.1016/j.ijbiomac.2019.09.003
0141-8130/© 2019 Elsevier B.V. All rights reserved.

In this context, PFL was immobilized on superparamagnetic $NiZnFe_2O_4$ octyl-nanoparticles coated with octyl group, producing the biocatalyst OCTYL-NANO-PFL.

To this goal, mixed nanoparticles (type $NiZnFe_2O_4$) were synthetized. This way, this composition of the metal blending has anti-corrosion properties [40] that can decrease the oxidation percentage of the nanoparticles. This improves the storage and operational stability of the biocatalyst [40,41]. The functionalization of superparamagnetic $NiZnFe_2O_4$ was performed with octyltriethoxysilane that generates a hydrophobic acyl layer where PFL may be immobilized via interfacial activation [18,19,30].

Although this lipase immobilization method has many advantages [18], it has a problem: the enzyme may be released during operation or when submitted to drastic conditions (high temperatures or the presence of cosolvents, substrate or products-like detergents) [18,42–45]. One solution to this problem is the immobilization of the enzyme on acyl-heterofunctional supports [44,46,47]. Other alternative is the physical crosslinking with PEI [48–50] or the covalent crosslinking using aldehyde dextran [51–55]. However, the use of small bifunctional crosslinking reagents may have some advantages, as they can confer not only some intermolecular crosslinking, but also some stabilizing intramolecular ones, that could increase enzyme rigidity [56].

Thus, in order to improve the stability of OCTYL-NANO-PFL, the immobilized PFL was chemical modified by different bifunctional molecules, namely: glutaraldehyde, divinylsulfone and *p*-benzoquinone. The chemical modification of immobilized enzymes is simpler and easier to control than that of the soluble enzymes and the final features of the immobilized enzyme may be greatly improved [57,58].

Glutaraldehyde (GA) is one of the most widely used reagents for enzyme crosslinking [59–64].This bifunctional reagent can mainly react with the primary amine groups of proteins [59], the reactivity depends on the number of GA molecules involved in the modification of the amine groups [63,65]. Divinylsulfone (DVS) also has been used for lipase immobilization [41,66–74]. DVS molecule is capable of reacting with primary (and secondary amines), phenyl, hydroxyl, thiol and imidazol groups of the enzyme surface and is very stable a broad range of pH values (from 5 to 10) [67,75]. *p*-Benzoquinone (BQ) can be used as an alternative to DVS, since the enzyme groups that can react with it are similar [76], and it has been recently compared to DVS as support activating reagent [41]. BQ has been used to produce magnetic cross-linked aggregates of lipase from *Yarrowia lipolytica* [77].

The chemical modification of a protein will have different effects on its features. The one point modification may alter the physical features of the enzyme surface, and that may have positive or negative effects on enzyme properties [57,58]. A positive effect on enzyme stability may be the intermolecular crosslinking, that can reduce enzyme release from the support [18,48,49,51,54,55], together to some possibilities of enzyme rigidification if many groups of different enzyme molecules are involved [55]. Intramolecular enzyme crosslinking can also produce an increment in the enzyme structure rigidity [56,63]. These inter or intra molecular crosslinkings may be difficult to achieve using these small bifunctional reagents, as they require that two reactive groups in the protein are placed at the correct distances and locations [18,48]. And although with glutaraldehyde it has been reported that there is not competition between one-point modification and crosslinking [59,63] that is not so clear using BQ or DVS.

2. Materials and methods

2.1. Materials

PFL as a powder with 6% (w/w) of protein content, 25% (v/v) GA aqueous solution, DVS, BQ, *p*-nitrophenyl butyrate (*p*-NPB) and octyltriethoxysilane (OTES) were purchased from Sigma Chemical Co (St. Louis, MO, USA). $FeCl_3.6H_2O$, $NiCl_2.6H_2O$ and $ZnCl_2$ were purchased from Dinâmica Química Contemporânea LTDA. All other reagents and solvents were of analytical grade.

2.2. Methodology

2.2.1. Preparation of octyl-nanoparticles

2.2.1.1. Synthesis of superparamagnetic $NiZnFe_2O_4$ nanoparticles. $NiZnFe_2O_4$ nanoparticles were prepared by hydrothermal synthesis [41,78,79]. In the procedure, an aqueous solution was prepared containing 0.74 M of $FeCl_3.6H_2O$, 0.185 M of $NiCl_2.6H_2O$ and 0.185 M of $ZnCl_2$, under vigorous mechanic stirring (6000 rpm). Subsequently, 10 mL of 35 mmol sodium hydroxide was added dropwise to precipitate the metal hydroxides. This mixture was transferred to a Teflon-lined autoclave at 250 °C during 30 min. Then, the precipitate was washed with distilled water until neutral pH and dried in a vacuum desiccator at room temperature at a pressure of 360 mmHg for a minimum of 48 h. The nanoparticles were stored under those conditions before their use.

2.2.1.2. Functionalization of $NiZnFe_2O_4$ nanoparticles with OTES. The procedure of nanoparticle functionalization was conducted according to Blanco et al. [80], with some modifications. 1 g of $NiZnFe_2O_4$ nanoparticles was suspended in 10 mL of OTES/toluene (1:4, v/v) solution. The suspension was gently stirred for 72 h at room temperature. After, the octyl-nanoparticles were washed twice with 20 mL of toluene, 3 times with 20 mL of hexane and 3 times with 20 mL of acetone. Finally, octyl-nanoparticles were dried in a vacuum desiccator during a minimum of 48 h at room temperature and a pressure of 360 mmHg. The nanoparticles were stored under those conditions before their use.

2.2.2. Characterization of nanoparticles

XDR analyses were performed using a Rigaku X-ray diffractometer equipped with CoKa radiation tube ($\lambda = 1.7889$ Å) operated at 30 kV and 15 mA. The phase identification of the sample was performed using standard patterns from the International Centre for Diffraction Data (ICDD). The diffraction pattern was refined by Rietveld procedure [81] using the DBWS 2.25 program [82]. The crystallite size of the nanoparticle was calculated using Scherrer's equation [83] from XDR data.

Fourier Transform Infrared Spectroscopy (FTIR) analyses were carried out on a Perkin Elmer spectrometer. For these experiments, the samples were previously mixed with KBr powder. The data were collected in the range of 400–4000 cm^{-1}.

The magnetic characterization of the nanoparticles was performed at room temperature using a vibrating sample magnetometer (VSM) Lakeshore 7400, with maximum magnetic field amplitude of 17 kOe. The VSM was previously calibrated using a pure nickel sample. Thus, after weighing each sample, the respective magnetization is given in emu/g.

2.2.3. Immobilization of PFL on octyl-nanoparticles

PFL was immobilized on octyl-nanoparticles (OCTYL-NANO) by interfacial activation [18,19], producing the biocatalyst OCTYL-NANO-PFL (Fig. 1). For that purpose, the PFL powder was dissolved in 5 mM sodium phosphate at pH 7, at a concentration of 20% powder w / v of solution. This enzyme solution was used for all studies. If required was diluted with 5 mM sodium phosphate at pH 7. In the immobilizations, 200 mg of the support was added into 2 mL of lipase solution (standard enzyme loading was 20 U/g support). The immobilization process was conducted under gentle stirring at room temperature. In some instances, a progressive increase of the enzyme concentrations was performed (from 20 U/g to 300 U/g). Fig. 1 shows the schematic preparation of the biocatalyst.

2.2.4. Chemical modification of OCTYL-NANO-PFL with GA, DVS and BQ

100 mg of the biocatalyst was suspended in 2 mL solutions of 200 mM sodium phosphate at pH 7 containing GA, DVS or BQ at

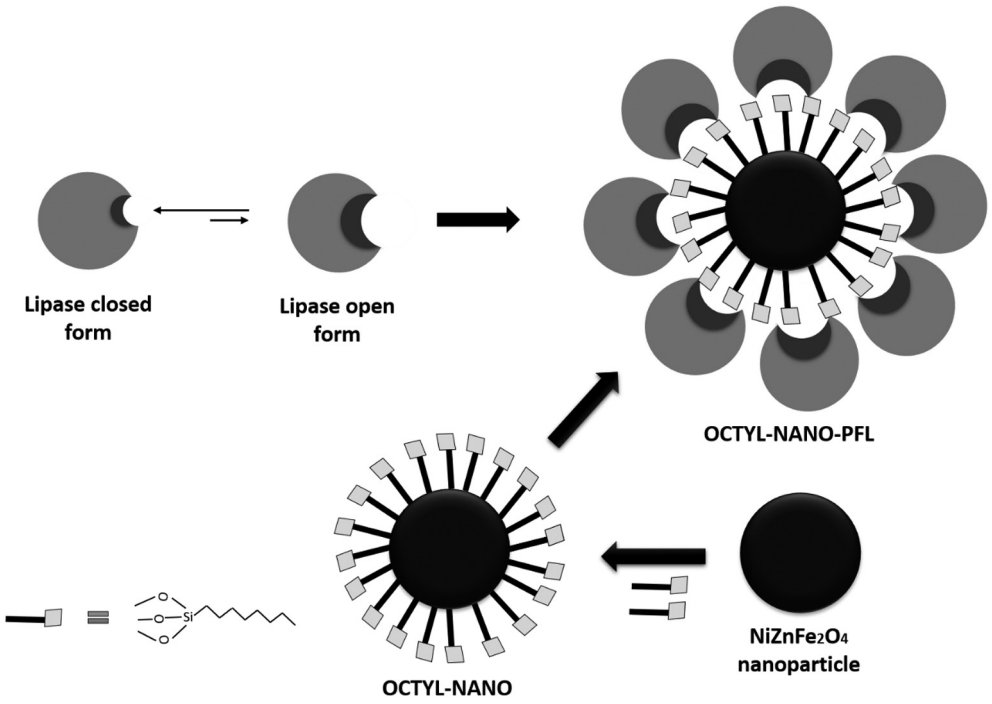

Fig. 1. Schematic representation of the production of OCTYL-NANO-PFL.

different concentrations (0.5, 1, 2.5 or 5% v/v (GA and DVS) or w/v (BQ) at room temperature for 1 h, under gentle stirring. The resulting modified biocatalysts were named mentioning the modificating agent and the concentration, e.g., OCTYL-NANO-PFL-GA 0.5%.

2.2.5. Determination of enzymatic activity and protein concentration

The enzymatic activity was quantified using *p*-nitrophenyl butyrate as substrate, according to the procedure related for Lombardo et al. [84]. The hydrolysis of *p*-NPB was conducted under gentle stirring, adding 50 μL of *p*-NPB solution (50 mM *p*-NPB in acetonitrile) to 2.5 mL of sodium phosphate buffer at pH 7 and 25 °C and the reaction was started adding 50 μL of sample. *p*-NPB was measured at 348 nm (isosbestic point, $\varepsilon_c = 5.236\ mol^{-1}.cm^{-1}$) [84]. In this work, one unit (U) is the amount of enzyme that was able to hydrolyze 1 μmol of substrate per minute under the described conditions. The amount of immobilized enzyme on the support was calculated using the ratio between the activity of supernatant of the immobilization suspension after the immobilization and the activity of a reference solution having the enzyme under identical conditions but without support. It is important to mention that the activity of the enzyme reference solution was maintained at 100% during all the immobilization process. The expressed activity was calculated using the ratio between the observed immobilized enzyme activity and the activity that was expected in the biocatalyst from the immobilization yield and the activity of the free enzyme.

Protein concentration was determined using Bradford method [85] and bovine serum albumin was used as the standard.

2.2.6. SDS-PAGE electrophoresis analyses

The SDS-PAGE analyses were carried out using 12% polyacrylamide gels [86] with an Miniprotean tetra-cell (Biorad) electrophoresis unit. The rupture buffer was prepared according to Garcia-Galan et al. [87]. In the procedure, 100 mg of immobilized enzyme were suspended in 1000 μL of rupture buffer, containing 4% (v/v) of SDS and 10% of mercaptoethanol. The samples were boiled during 10 min at 100 °C and after centrifugation at 6000 rpm in Eppendorf centrifuge, 15 μL of the supernatants were injected in the electrophoresis unit. The low molecular weight marker of proteins (LMW-SDS Marker — GE Healthcare LifeSciences) was used as standard.

To stain the gel, it was washed with a solution of 30% (v/v) ethanol and 2% (w/v) of phosphoric acid, 3 times for 30 min. After, the gel was washed 3 times during 20 min with a solution of 2% (w/v) of phosphoric acid. Subsequently, the gel was incubated during 30 min in 100 mL of a solution containing 18% (v/v) ethanol, 2% (w/v) of phosphoric acid and 15% (w/v) of ammonium sulfate. Finally, it was added 1 mL of 2% (w/v) Coomassie brilliant blue. This Coomassie solution was in contact with the gel at room temperature during 24 h, under mild stirring.

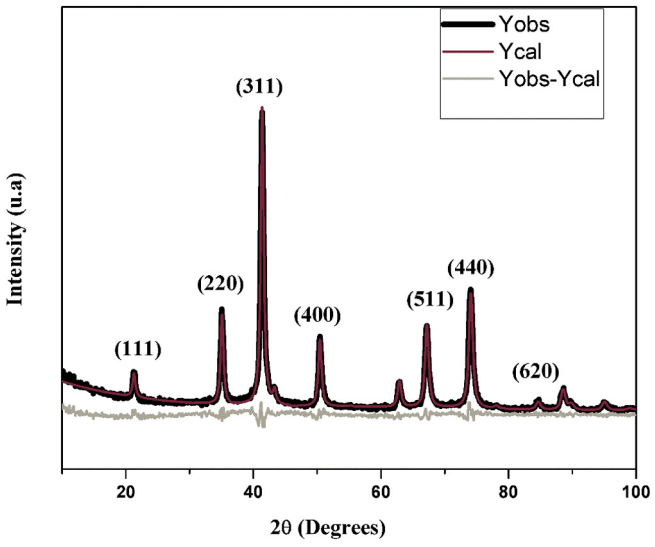

Fig. 2. XRD pattern of the $NiZnFe_2O_4$ nanoparticles. The black line represents the experimental data (Yobs), the dark gray line represents calculated intensities obtained through the refinement (Ycal) and the light gray line represents the relative difference between experimental and calculated data (Yobs-Ycal).

Table 1
Structural parameters of the $NiZnFe_2O_4$ nanoparticles obtained from Rietveld refinement.

Sample	Lattice parameters (a) (A)	Rwp (%)	S	Average crystalline size (nm)
$NiZnFe_2O_4$	8.4073	11.59	0.92	20

2.2.7. Stress inactivation of different PFL biocatalysts

A mass of 1.0 g of immobilized preparations was suspended in 5 mL of 25 mM buffer solutions (sodium citrate at pH 5, sodium phosphate at pH 7, sodium carbonate-bicarbonate at pH 9) at 60 °C. Periodically, samples were withdrawn and the activity versus *p*-NPB was measured as described above. The enzymatic deactivation course was built using the initial activity as 100% and the half-life ($t_{1/2}$) for each immobilized enzyme preparation was calculated according to Sadana and Henley [88], using a Microcal Origin program, version 8.1.

2.2.8. Capture and reuse of the magnetic biocatalysts

A mass of 10 mg of biocatalyst was utilized to perform consecutive cycles of 12 min of *p*-NPB hydrolysis under the conditions described above. At the end of each cycle, the biocatalyst was washed 2 times with 10 mL of 25 mM sodium phosphate at pH 7, recovering the biocatalysts by using a magnet. Thus, the relative activity of the biocatalyst in each cycle was calculated, taking as 100% the activity in the first cycle of *p*-NPB hydrolysis.

3. Results and discussion

3.1. Characterization of superparamagnetic $NiZnFe_2O_4$ nanoparticles before and after enzyme immobilization

The physical and magnetic properties of the biocatalyst and the nanoparticles were studied using XRD, FTIR and VSM. A deeper characterization of $NiZnFe_2O_4$ nanoparticles is in a recently publication of our group [79]. In this report, we studied the effects of the NaOH content and reaction time on the growth mechanism, as well as structural, morphological and magnetic properties of $NiZnFe_2O_4$ nanoparticles. Once we employed the same synthetic methodology and composition, the morphology is the same as the particles presented in our previous publication. Additionally, we coated the magnetic nanoparticles just with compounds based on organic matter, as consequence the morphology of the inorganic part did not change.

The XRD analysis permitted to obtain data on the crystalline phase and structural parameters of $NiZnFe_2O_4$ nanoparticles. The pattern shows the reflection planes (111), (220), (311), (400), (440), (511) and (620) (Fig. 2), that can be indexed as to the inverse spinel structure $NiZnFe_2O_4$ (ICSD/PDF-08-4611) [89,90]. From the refinement of the data from XRD, it was possible to identify a single phase for the sample. The structural parameters obtained through Rietveld refinement are summarized in Table 1. The low values founded for the R_{WP} and the proximity of *S* of one value show that the refinement was satisfactory [78]. The lattice parameter (a, b and c) obtained in this work are in agreement with other $NiZnFe_2O_4$ nanoparticles preparations described in literature [78,90,91]. The average crystalline size, which relates the crystallite size with the half-width of the diffraction peak, presented

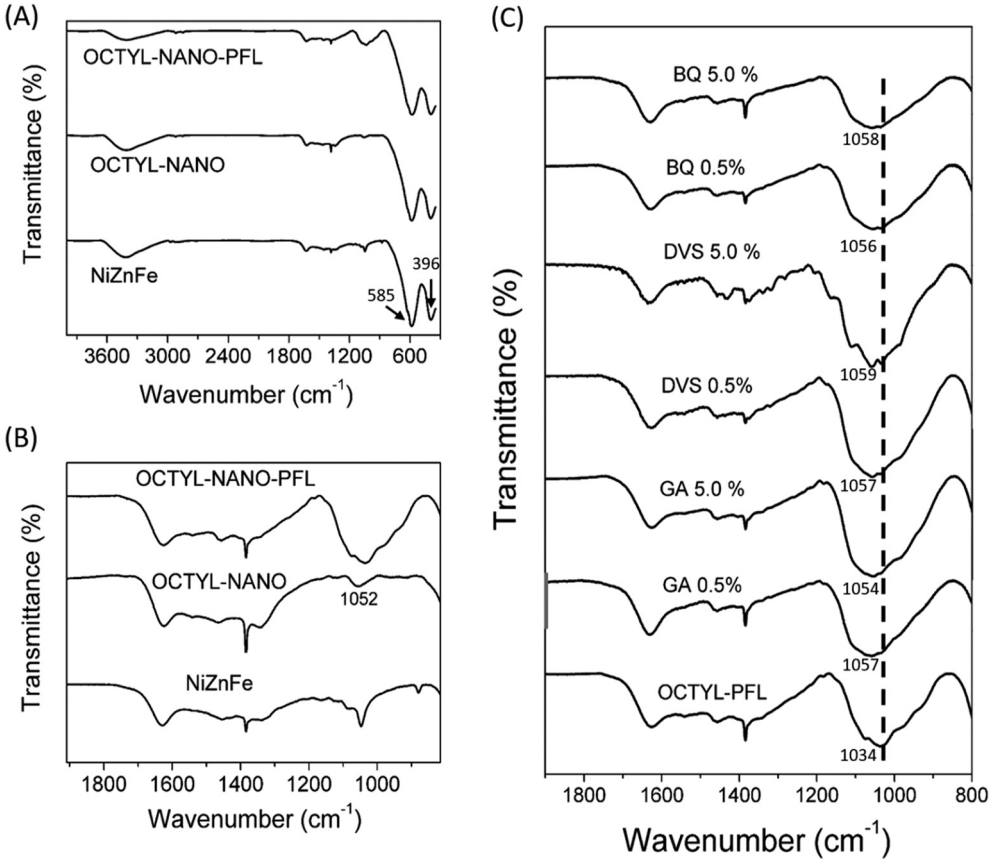

Fig. 3. FTIR spectra of different nanoparticle samples. (A) Full (4000 to 350 cm^{-1}) and (B) extended (1900 to 800 cm^{-1}) FTIR spectra for NiZnFe, OCTYL-NANO and OCTYL-NANO-PFL samples. (C) Extended FTIR spectra of the modified biocatalysts.

Table 2
Vibrational modes of FTIR spectra of NiZnFe2O4 nanoparticles. Stretching vibration (ν) and bending vibration (δ).

Wavenumber (cm^{-1})	Vibration mode	Description
396	νFe–O and νNi–O	Vibration of Fe—O and Ni—O bonds in octahedral sites
585	νFe–O and νZn–O	Vibration of Fe—O and Zn—O bonds in tetrahedral sites
1052	δSi–O	Vibration of Si—O bonds in silane molecules
1390	δC–H	Vibration of CH_3 groups

Table 3
Magnetic properties of the different samples.

Sample	M_S (emu/g)	Mr (emu/g)	Hc (Oe)
NiZnFe	86.8	4	17.7
OCTYL-NANO	58.6	1.55	8.62
OCTYL-NANO-PFL	58.2	2.85	7.8
OCTYL-NANO-PFL-GA 0.5%	58.5	1.48	7.45
OCTYL-NANO-PFL-GA 5%	56.5	2.2	13.8
OCTYL-NANO-PFL-DVS 0.5%	57.8	2.4	14.6
OCTYL-NANO-PFL-DVS 5%	57.2	1.5	8.15
OCTYL-NANO-PFL-BQ 0.5%	58.1	1.1	6.7
OCTYL-NANO-PFL-BQ 5%	57.5	2.1	11

values below of 30 nm, indicating of superparamagnetism properties of these materials [92]. The relation between size and superparamagnetism behavior of magnetic nanoparticles can be seen in Eq. (1) [93,94]:

$$T_B = \frac{KV}{25k_B} \quad (1)$$

where, K is the contribution of uniaxial anisotropy, V is the volume of the NPs and k_b is Boltzmann constant. T_B is the blocking temperature, which is the temperature that the thermal energy overcomes all barrier energies necessary to demagnetize the nanoparticles. Therefore, our goal is to obtain nanoparticles with blocking temperatures below operating temperature. i. e., with superparamagnetic behavior at room temperature. In the Eq. (1), it is possible to observe that the smaller the nanoparticle volume, which is related to the size of the nanoparticle, the lower the blocking temperature. For this reason, magnetic materials with superparamagnetism behavior must have its dimensions in the nanoscale regime.

FTIR gave information on the modification surface of the superparamagnetic $NiZnFe_2O_4$ nanoparticles. All samples presented two bands in the range of 396–585 cm^{-1}, which were assigned to the vibration of ions in the crystal lattice of $NiZnFe_2O_4$ nanoparticles (Fig. 3(A)). The 585 cm^{-1} band was attributed to stretching vibration of Fe—O and Zn—O bonds in tetrahedral sites, whereas the band in 396 cm^{-1} is relative to stretching vibration of Fe—O and Ni—O bonds in octahedral sites (Table 2) [95].The FTIR spectrum of OCTYL-NANO sample showed an band in the 1052 cm^{-1}, which is relative to bending vibration of Si—O bonds [96].

The FTIR spectrum of the sample OCTYL-NANO-PFL exhibited new bands in 1625, 1456 and 1405 cm^{-1}, which can be attributed to vibrational modes of amides functional groups [97] of the enzyme. However, these bands cannot be used to prove PFL immobilization, once there are vibrational modes at the same wavenumbers for the sample NiZnFe that are probably due to hydroxyl groups on the surface of NiZnFe nanoparticles or CO_2 interference [98]. Nevertheless, the set of bands in the region between 868 and 1162 cm^{-1} for the sample OCTYL-NANO-PFL clearly indicates the PFL immobilization. This band can be attributed to the C—N stretching (ν_{C-N}), C—H bending (δ_{C-H}), CH_2 wagging (γ_{CH2}), or C—O stretching (ν_{C-O}), of the amino acid side chains in PFL [99,100]. However, the best way to show immobilization is to show the enzyme activity incorporated to the support, as we will see in the next section.

The FTIR spectra for the biocatalysts samples modified with GA, DVS and BQ are similar to that of OCTYL-NANO-PFL sample, as shown in Fig. 3(C). For these samples, no additional vibrational modes were evidenced. However, the set of bands (ν_{C-N}, δ_{C-H}, γ_{CH2}, ν_{C-O}) in the modified samples sifted to 1054–1059 cm^{-1} (with respect to 1034 cm^{-1} for OCTYL-NANO-PFL), as shown in Fig. 3(C). The literature reports that the wave-numbers of some FTIR vibrational modes of proteins are sensitive to structural conformational changes [101]. Therefore, the shift evidenced in the FTIR spectra for the modified biocatalysts indicates that the chemical modification could induce some structural conformational changes in the immobilized PFL. This was later evidenced by functional changes on the biocatalyst.

The VSM curves at room temperature were used to evaluate the magnetic properties of the materials prepared herein. Fig. 4-A shows that the functionalization with octyltriethoxysilane decreased the saturation magnetization (M_S), from 86.8 emu/g for NiZnFe nanoparticles to 58.6 emu/g for OCTYL-NANO, due to the presence of non-magnetic material on the nanoparticle. The PFL immobilization on the nanoparticle induced a slightly effect in the M_S values, a reduction from 58.6 emu/g

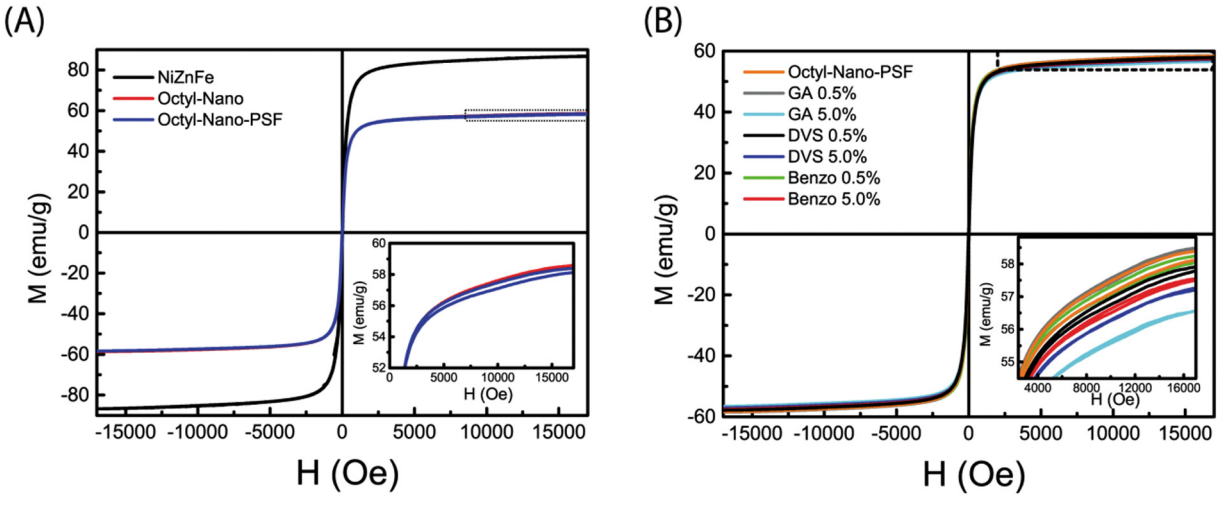

Fig. 4. VSM curves for (A) NiZnFe nanoparticle, OCTYL-NANO and OCTYL-NANO-PFL samples and (B) chemically modified biocatalysts.

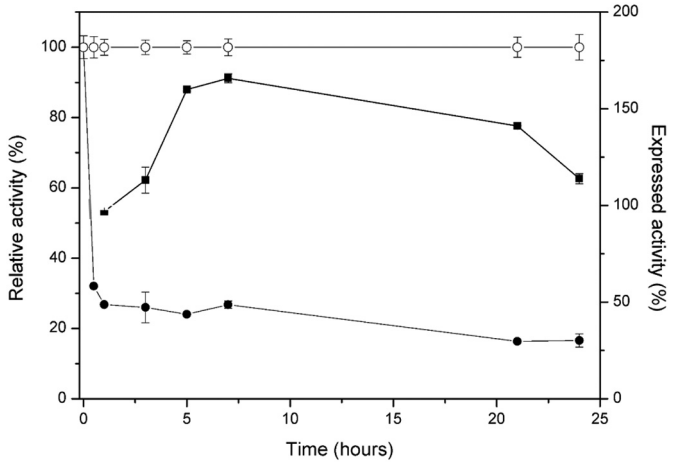

Fig. 5. Immobilization course of PFL on OCTYL-NANO. Relative total activities of reference (○) and supernatant (●) during immobilization and expressed activities during immobilization (■). The lines represent the tendency of experimental data. 100% is taken as the initial activity of PFL in both cases.

to 58.2 emu/g (perhaps due to the low enzyme loading). Additionally, it has evidenced a slightly decrease of M_S with the increasing of the amount of bifunctional agent (Fig. 4-B – inset), for the same reason of the decreasing in the sample OCTYL-NANO.

Table 3 summarizes the values of M_S, coercive field (H_C) and remnant magnetization (M_r) for all materials prepared in this work. The small values of H_C and M_r indicate that the prepared magnetic biocatalysts are in the superparamagnetic (SPM) regime at room temperature. This is an important feature for a magnetic biocatalyst, once the SPM regime avoids magnetic interparticle self-aggregation during biocatalysts operational use. This aggregation will produce macroporous aggregates, that can reduce substrate accessibility and consequently decrease the reaction rate [102,103], and are not pursued in this paper. Furthermore, all biocatalysts presented a relatively great M_S (>56 emu/g), which enable a rapid magnetic separation.

It is worth to further mention the important selection of NiZn ferrite as magnetic support for enzymes. Naked NiZn nanoparticles presented a high magnetization saturation (86.8 emu/g – see Table 3), which is related to fine tuning of the chemical concentration of Ni^{2+} and Zn^{2+} on the crystal structure of the nanoparticles. Cations in spinel ferrites occupy two sites: tetrahedral (A sites) and octahedral (B sites). In *inverse* spinels, the divalent ion occupies the B sites and trivalent ions occupy both A and B sites. As a consequence, the magnetic moment of inverse spinel ferrites comes from divalent ions. In *normal* spinel ferrites (such as Zn ferrite) divalent ion occupy the A site, which makes the magnetic moment of the spins of Fe^{3+} in B site to be anti-parallel and no net magnetization. However, when Zn^{2+}, at certain concentration, are in mixed Ni ferrites, the net magnetic moment in B sites increases, due to the presence of Fe^{3+} ions, which enhances the magnetization saturation of the nanoparticle [104]. Therefore, the choice of this support caused that, even after a high loading of non-magnetic matter, the biocatalyst possess enough remaining magnetization to be magnetically separated from the reaction medium In addition, greater protection against oxidation is achieved due to Fe^{2+} replacement.

3.2. Immobilization of PFL on octyl-nanoparticles

PFL was immobilized on OCTYL-NANO by interfacial activation [18,19], producing the biocatalyst OCTYL-NANO-PFL (Fig. 1). The immobilization course is shown in Fig. 5.

Most lipase activity was immobilized on OCTYL-NANO in the first hour of contact, since the activity of supernatant rapidly decreased while the reference enzyme solution maintained intact its activity during all immobilization time. In 1 h of contact, immobilization yield is about 74%. The immobilization yield reached a value over 83% after 24 h.

Fig. 5 also shows an increase of the activity of the immobilized enzyme (until 7 h of immobilization), achieving about 140–160% of initial activity. That is, the immobilized enzyme was more active than the free enzyme and the final biocatalysts presented more activity versus *p*-NPB per mg of enzyme, as expected if immobilization is via interfacial activation. This may be explained by the immobilization of the lipase vis its open and monomeric form [18,19,46,105–109] PFL-PFL dimer have lower activity than the monomeric enzyme [110–113]. For this reason, we have neither used the free enzyme as reference for these studies.

3.3. Chemical modification of OCTYL-NANO-PFL with GA, DVS and BQ

The immobilized enzyme was modified with GA, DVS and BQ and the effects of the concentration of these reagents on the activity retention and thermal stability were investigated.

Table 4 shows the activities and half-lives of OCTYL-NANO-PFL modified with different concentrations of GA, DVS or BQ. The chemical modification of an enzyme is expected to alter the enzyme activity, because it may alter the enzyme conformation or modify some critical groups for enzyme activity (e.g., the catalytic Ser). Thus, usually the chemical modification is expected to produce some decrease in enzyme activity. In fact, the PFL preparations decreased their activities after the treatment with GA, DVS or BQ, except when using 1% GA, where an increased activity (by 18%) was observed (even although 0.5% GA was quite negative for enzyme activity). This worse effect of intermedium chemical modifications of immobilized enzymes on enzyme activity when compared with full modifications has been reported in other cases [63,87,114,115].

Table 4
Effect of different treatments on activity and stability of the PFL immobilized preparations. Activity values are given as relative activity and the stability factor were calculated considering the unmodified biocatalyst as a 100%. Inactivation conditions: 60 °C, 25 mM sodium phosphate buffer at pH 7.

Biocatalyst	Relative activity (%)	Half-lives (min)	Stabilization factor
OCTYL-NANO-PFL	100 ± 0	10.81	1
OCTYL-NANO-PFL-GA 0.5%	56.61 ± 2.66	475.66	44.00
OCTYL-NANO- PFL-GA 1%	118.67 ± 1.96	349.39	32.32
OCTYL-NANO- PFL-GA 2.5%	60.97 ± 1.27	455.39	42.13
OCTYL-NANO- PFL-GA 5%	75.48 ± 0.22	649.69	60.10
OCTYL-NANO- PFL-DVS 0.5%	70.01 ± 5.41	84.29	7.80
OCTYL-NANO- PFL-DVS 1%	85.16 ± 5.97	652.35	60.35
OCTYL-NANO- PFL-DVS 2.5%	70.08 ± 3.10	302.08	27.94
OCTYL-NANO- PFL-DVS 5%	66.28 ± 5.23	14.12	1.31
OCTYL-NANO- PFL-BQ 0.5%	71.67 ± 4.31	90.74	8.39
OCTYL-NANO- PFL-BQ 1%	59.95 ± 1.01	36.29	3.36
OCTYL-NANO- PFL-BQ 2.5%	62.41 ± 2.70	28.08	2.60
OCTYL-NANO- PFL-BQ 5%	57.73 ± 6.92	50.42	4.66

However, when focusing on PFL stability, most chemical modifications (at all concentrations) improved the stability of the immobilized biocatalyst. GA modification produced the highest stabilization factors (ranging from 32 to 60), being the biocatalyst OCTYL-NANO-PFL-GA 5% the most stable one. Although we can expect that almost in all cases at least one molecule of glutaraldehyde has reacted with one amino group, producing a certain hydrophobization on the enzyme, modifying its stability [63,114,116], the stabilization could be caused by the promotion of inter or intermolecular crosslinkings, as amino-glutaraldehyde groups are very reactive with other amino – glutaraldehyde groups [50,63,117].

DVS molecule can react with different moieties of the protein, namely amine, hydroxyl, phenyl, thiol and imidazol groups [67,75]. However, the stabilization obtained with this reagent is lower than using GA, except using 1% DVS, where results become similar to those obtained using 5% GA. Modifications with concentrations over 1% DVS decreased the stability of the immobilized protein. These negative effects are evident in the OCTYL-NANO-PFL-DVS 5%, since the stability of this biocatalyst is almost identical to the unmodified biocatalyst. These results can be caused by a combination of negative effects of the one point chemical modification on the enzyme stability, the positive effects of inter or intramolecular crosslinkings, and a difficulty of reaction between two vinylsulfone groups attached to the enzyme, that make complex the crosslinking promotion when all enzyme reactive groups are modified with DVS.

Chemical modification with BQ was the one offering the lowest stabilization factors (Table 4). BQ can react with the same groups of the protein than DVS [76,118]. The biocatalyst OCTYL-NANO-PFL-BQ 0.5% was the most stable among the BQ preparations (a factor of 8), but far for the stabilization factors obtained using GA or DVS. This suggested that the conditions for using BQ for crosslinking must be even more carefully selected that using DVS, apparently it is more difficult to have good stabilizations, although a more negative effect of the one point chemical modification cannot be secluded.

3.4. Effect of inactivation pH on the stability of the different PFL biocatalysts

Fig. 6 shows the inactivation courses of PFL immobilized preparations submitted to different conditions of pH.

The results from the Fig. 6A shows there are no significant effect of pH on the stability of OCTYL-NANO-PFL, since the half-lives remained around 11 min in all range of pH values studied. Other authors showed similar behavior of lipase from *Pseudomonas cepacia* immobilized onto electrospun polyacrylonitrile (PAN) nanofibrous membrane in relation to pH stability [119]. However, the enzyme immobilized on octyl agarose was significantly more stable at pH 5 than at pH 7 or 9 [46].

The chemical modification of OCTYL-NANO-PFL altered this situation. We show some representative examples, including always the preparation with the highest stability at pH 7 (Table 4).

Fig. 6B shows the inactivation courses of GA (using 0.5 and 5% GA) modified preparations. The results show that using 5% GA in the modification it is possible to get the highest stability at pH 5 (residual activity over 65% after 24 h), while using 0.5% GA the half-life of the biocatalyst was only 107 min. GA modified preparations also

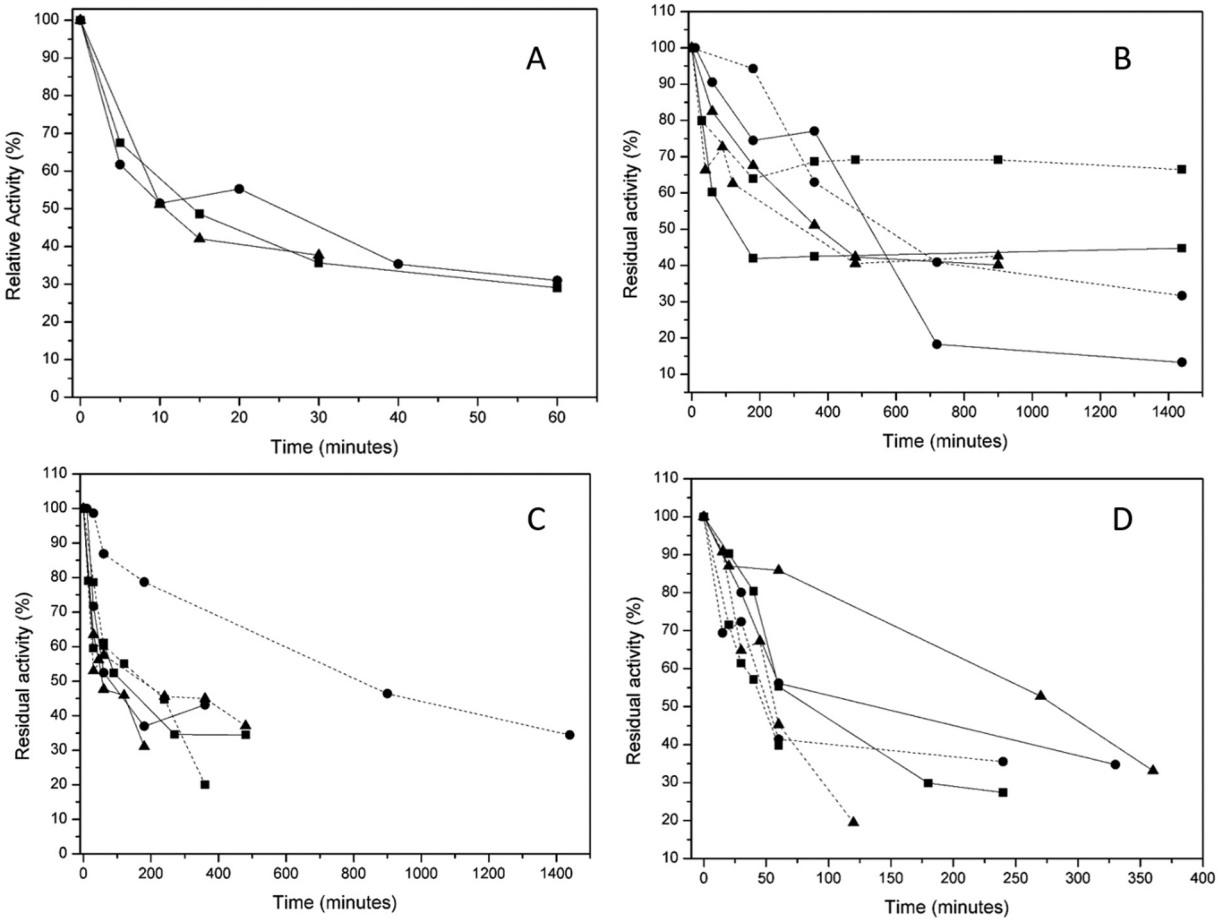

Fig. 6. Inactivation courses of differently modified OCTYL-NANO-PFL at 60 °C at different pH values. Unmodified biocatalyst (A); -GA 0.5% modified biocatalyst – solid lines and -GA 5% modified biocatalyst – dashed lines (B); -DVS 0.5% modified biocatalyst – solid lines and -DVS 1% modified biocatalyst – dashed lines (C); -BQ 0.5% modified biocatalyst – solid lines and- BQ 5% modified biocatalyst – dashed lines (D). Experiments have been performed in sodium citrate buffer at pH 5 (■), sodium phosphate buffer at pH 7 (●) and sodium carbonate-bicarbonate buffer at pH 9 (▲).

present high stability at pH 7 (half-lives about 475 and 650 min for 0.5 and 5% of GA, respectively). This is remarkable because phosphate ions have a negative effect on many lipases stability [120], including PFL [46]. It can be observed that the increase in the GA concentration (0.5 to 5%) had a negative effect on the biocatalyst stability at pH 9 (half-lives decreased from about 360 to 197 min for 0.5 and 5% of GA, respectively). This results show the complexity of the effect of the chemical modification, while at pH 5 and pH 7 the best modification is using 5% GA, at pH 9 the highest stability was found when modifying the immobilized enzyme using 0.5% GA. This could be founded on different inactivation pathways under different conditions [121], the different effects of the one point chemical modification when changing the inactivation conditions [121], even on the different solution that the modification offer to the negative effects of phosphate ions on enzyme stability [120].

Fig. 6C presents the inactivation courses of DVS modified preparations (using 0.5 and 1% DVS). The inactivation courses of OCTYL-NANO-PFL-DVS 0.5% remained almost unaltered when changing the inactivation pH, while OCTYL-NANO-PFL-DVS 1% stability was quite depended on the inactivation pH. This biocatalyst gave the highest stability (about 650 min) at pH 7 (again, even in the presence of phosphate ions [120]). At pH 5, the 1% of DVS modified preparation showed the highest stability (half-lives were about 72 and 121 min for modification in 0.5 and 1% of DVS, respectively). At pH 9, both DVS preparations presented similar stabilities, (half-lives were about 57 and 49 min for modification in 0.5 and 1% of DVS, respectively).

OCTYL-NANO-PFL modification with 0.5% of BQ produced the highest effect on enzyme stability when inactivated at pH 9, among the BQ modified preparations (half-life about 227 min, see Fig. 6D). The biocatalyst OCTYL-NANO-PFL-BQ 5% presented quite similar behavior with variation of the pH values (half-lives: 45.3, 50.4 and 66.6 min at pH 5, 7 and 9, respectively – see Fig. 6D).

Thus, stabilization factors achieved by the chemical modification depended on the inactivation pH. At pH 5, the stabilization factors are higher than 130 using OCTYL-NANO-PFL-GA 5% (and this factor compared 50% residual activity at pH 7 versus 68% at pH 5, we can guess that the stabilization factor will be over 200), higher than the 60 fold factor found at pH 7. Using 1% DVS in the modification, the stabilization in inactivations at pH 9 dropped from 60 at pH 7 to 11. Using BQ, the situation was different, and stabilization factors gone from just over 8 at pH 7 to >20 at pH 9. All these differences on the modification effects when changing the inactivation pH may be founded on the different factor commented above.

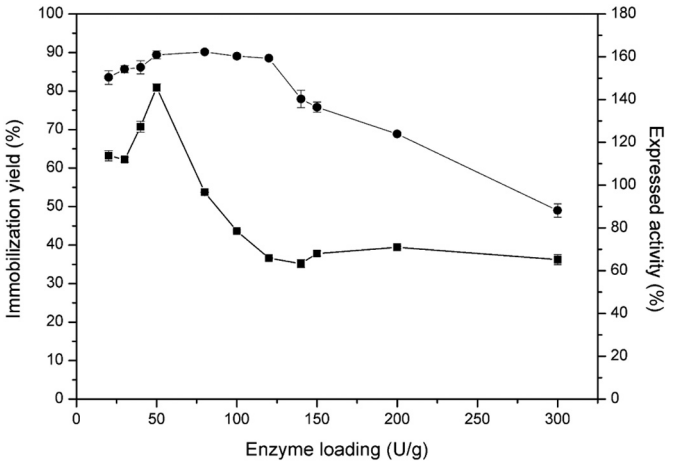

Fig. 7. Loading capacity of PFL on octyl-nanoparticles. Immobilization yield (●) and expressed activity (■).

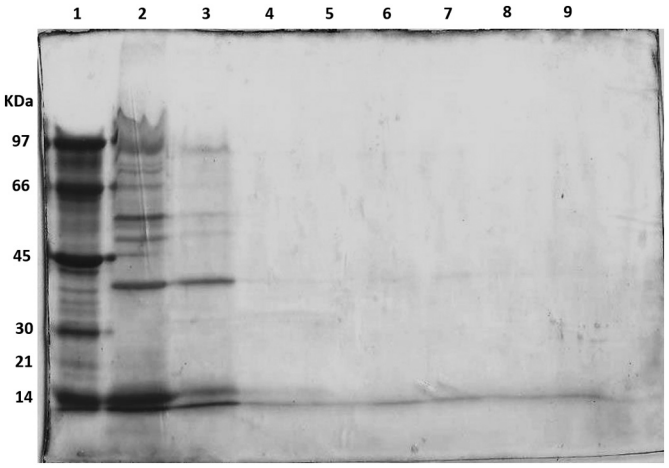

Fig. 8. SDS-PAGE gels of different PFL immobilized preparations. Lane 1: Molecular weight marker; Lane 2: soluble PFL; Line 3: unmodified biocatalyst (OCTYL-NANO-PFL); Lane 4: OCTYL-NANO-PFL-GA 0.5%; Lane 5: OCTYL-NANO-PFL-GA 5%; Lane 6: OCTYL-NANO-PFL-DVS 0.5%; Lane 7: OCTYL-NANO-PFL-DVS 1%; Lane 8: OCTYL-NANO-PFL-BQ 0.5%; Lane 9: OCTYL-NANO-PFL-BQ 5%.

3.5. Loading capacity of OCTYL-NANO for PFL immobilization

This parameter is an important feature of the support, mainly for industrial applications of biocatalyst produced. In this context, the immobilization of growing amounts of PFL on octyl-nanoparticles to produce the biocatalyst OCTYL-NANO-PFL was investigated. Fig. 7 shows that the maximum loading capacity of our new support is 200 U/g or 8.8 mg enzyme/g of support. However, the expressed activity did not follow the same patter. It increased until 50 U/g, which gave 145% expressed activity and then decreased with the increase of enzyme loading, the expressed activity become about 70% when offering 150 U/g. Other authors also reported the decreased of catalytic efficiency in the high loading lipase immobilization on magnetic nanoparticles [122–124], perhaps because now the substrate must diffuse by the holes between enzyme molecules to reach the active center, as the active center is on the support surface [125].

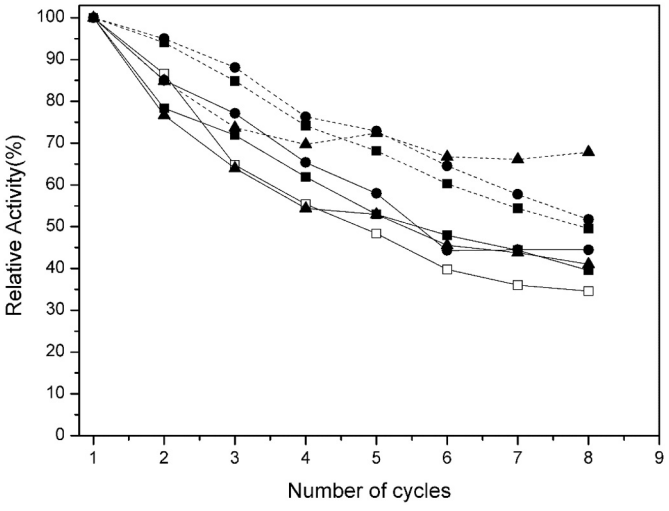

Fig. 9. Reuse of different immobilized PFL magnetic biocatalyst in the hydrolysis of *p*NPB 1 mM. OCTYL-NANO-PFL: Solid line (□); OCTYL-NANO-PFL-GA 0.5%: Dashed line (●); OCTYL-NANO-PFL-GA 5%: Solid line (●); OCTYL-NANO-PFL-DVS 0.5%: Dashed line (■); OCTYL-NANO-PFL-DVS 1%: Solid line (■); OCTYL-NANO-PFL-BQ 0.5%: Dashed line (▲); OCTYL-NANO-PFL-BQ 5%: Solid line (▲).

3.6. SDS-PAGE analysis of immobilized preparations

The SDS-PAGE analyses of some highly loaded PFL immobilized and modified preparations were performed in order to verify the effectiveness of the enzyme inter molecular crosslinking (Fig. 8). OCTYL-NANO-PFL sample (lane 3) gave a protein band corresponding to PFL (that was desorbed from the support under the conditions used in the sample preparation, boiling in SDS). After the chemical modifications used in this paper, the band of the PFL is no longer visible (lanes 4 to 9), indicating the establishment of a massive intermolecular crosslinking, since no protein was released from the support.

3.7. Repetitive capture of the different OCTYL-NANO-PFL particles

One of the problems of the magnetic nanoparticles is the real capture of the materials during operation, which may be related to difficulties in capture or particle breakage. To check this, several cycles of *p*-NPB hydrolysis using mechanical stirring (150 rpm) were performed reusing the same biocatalysts.

Fig. 9 shows that the activity of OCTYL-NANO-PFL decreased along the reaction cycles, with a 35% of recovered activity after 8 cycles. This was attributed mainly to two causes; enzyme release from the support during operation and the breaking of the nanoparticles, that reduce the amount of catalysts captured in each operation (the nanoparticles fragments are no longer magnetic and will be washed way).

All chemically modified biocatalysts had operational stabilities greater than the unmodified biocatalyst. Without discarding a likely positive effect on increase of the mechanical resistance of the biocatalyst due to crosslinking, and the role of improved enzyme stability, the main reason for this could be founded in the reduction of enzyme release from these modified biocatalysts (Fig. 8).

OCTYL-NANO-PFL-BQ 0.5% retained about 70% of its activity after 8 cycles of reaction, followed by OCTYL-NANO-PFL-GA 0.5% and -DVS 0.5% biocatalysts, with about 50% of their activities in the last cycle.

These biocatalysts were operationally more stable than TLL covalent immobilized on superparamagnetic nanoparticles prepared in the hydrolysis of *p*-NPB (*p*-NPB can also have some negative effect on enzyme stability) [99].

4. Conclusion

The results of this study show that lipase from *Pseudomonas fluorescens* was immobilized on octyl-nanoparticles, with expressed activities about 150%, suggesting the interfacial activation of the lipase, fixing the open form of the adsorbed lipase molecules. Furthermore, the chemical modification of this biocatalyst with different bifunctional reagents has been performed improving the enzyme stability and, in certain cases, even activity. The inactivation pH also affected very differently the stabilities of the different biocatalysts, suggesting the complexity of the effects. The intermolecular crosslinking was clearly evidenced by the lack of enzyme release even under very drastic conditions (boiling in SDS during SDS-PAGE samples preparation), increasing enzyme stability. Among these biocatalysts, OCTYL-NANO-PFL-GA 5% was the most thermally stable biocatalyst at pH 5, since its half-life was over 24 h at 60 °C (residual activity over 65% after 24 h of inactivation).

Acknowledgements

The authors thanks for the CAPES (Finance Code 001), CNPq (408790/2016-4) and FUNCAP (PNE-0112-00048.01.00/16, BP3-0139-00005.01.00/18) for financial support. Authors also thank MICIU (Ministerio de Ciencia, Innovacion y Universidades) by the support (project CTQ2017-86170-R). Nathalia S. Rios thanks to CNPq for a predoctoral fellowship (CNPq scholarship—Brazil).

References

[1] A. Salihu, M.Z. Alam, Solvent tolerant lipases: a review, Process Biochem. 50 (2015) 86–96, https://doi.org/10.1016/j.procbio.2014.10.019.
[2] K.E. Jaeger, M.T. Reetz, Microbial lipases from versatile tools for biotecnology, Trends Biotechnol. 16 (1998) 396–403, https://doi.org/10.1016/S0167-7799(98)01195-0.
[3] R.D. Schmid, R. Verger, Lipases: interfacial enzymes with attractive applications, Analysis. 37 (1998) 1608–1633, https://doi.org/10.1002/(SICI)1521-3773(19980703)37:12<1608::AID-ANIE1608>3.0.CO;2-V.
[4] B.R. Facin, M.S. Melchiors, A. Valério, J.V. Oliveira, D. De Oliveira, Driving immobilized lipases as biocatalysts: 10 years state of the art and future prospects, Ind. Eng. Chem. Res. 58 (2019) 5358–5378, https://doi.org/10.1021/acs.iecr.9b00448.
[5] S. Hama, H. Noda, A. Kondo, How lipase technology contributes to evolution of biodiesel production using multiple feedstocks, Curr. Opin. Biotechnol. 50 (2018) 57–64, https://doi.org/10.1016/j.copbio.2017.11.001.
[6] B.P. Dwivedee, S. Soni, M. Sharma, J. Bhaumik, J.K. Laha, U.C. Banerjee, Promiscuity of lipase-catalyzed reactions for organic synthesis: a recent update, ChemistrySelect 3 (2018) 2441–2466, https://doi.org/10.1002/slct.201702954.
[7] A. Tarczykowska, A. Sikora, M.P. Marszall, Lipases-valuable biocatalysts in kinetic resolution of racemates, Mini Rev. Org. Chem. 15 (2017) 374–381, https://doi.org/10.2174/1570193x15666171228145012.
[8] N. Sarmah, D. Revathi, G. Sheelu, K. Yamuna Rani, S. Sridhar, V. Mehtab, C. Sumana, Recent advances on sources and industrial applications of lipases, Biotechnol. Prog. 34 (2018) 5–28, https://doi.org/10.1002/btpr.2581.
[9] M.B. Ansorge-Schumacher, O. Thum, Immobilised lipases in the cosmetics industry, Chem. Soc. Rev. 42 (2013) 6475–6490, https://doi.org/10.1039/c3cs35484a.
[10] P. Adlercreutz, Immobilisation and application of lipases in organic media, Chem. Soc. Rev. 42 (2013) 6406–6436, https://doi.org/10.1039/c3cs35446f.
[11] F. Secundo, G. Carrea, C. Tarabiono, P. Gatti-Lafranconi, S. Brocca, M. Lotti, K.-E. Jaeger, M. Puls, T. Eggert, The lid is a structural and functional determinant of lipase activity and selectivity, J. Mol. Catal. B Enzym. 39 (2006) 166–170, https://doi.org/10.1016/j.molcatb.2006.01.018.
[12] C. Carrasco-López, C. Godoy, B. de las Rivas, G. Fernández-Lorente, J.M. Palomo, J.M. Guisán, R. Fernández-Lafuente, M. Martínez-Ripoll, J.A. Hermoso, Activation of bacterial thermo alkalophilic lipases is spurred by dramatic structural rearrangements, J. Biol. Chem. 284 (2009) 4365–4372, https://doi.org/10.1074/jbc.M808268200.
[13] A.M. Brzozowski, U. Derewenda, Z.S. Derewenda, G.G. Dodson, D.M. Lawson, J.P. Turkenburg, F. Bjorkling, B. Huge-Jensen, S.A. Patkar, L. Thim, A model for interfacial activation in lipases from the structure of a fungal lipase-inhibitor complex, Nature 351 (1991) 491–494, https://doi.org/10.1038/351491a0.
[14] H. Van Tilbeurgh, M.P. Egloff, C. Martinez, N. Rugani, R. Verger, C. Cambillau, Interfacial activation of the lipase-procolipase complex by mixed micelles revealed by X-ray crystallography, Nature 362 (1993) 814–820, https://doi.org/10.1038/362814a0.
[15] W.A. Hide, L. Chan, W.-H. Li, Structure and evolution of the lipase superfamily, J. Lipid Res. 33 (1992) 167–178http://www.ncbi.nlm.nih.gov/pubmed/1569370.
[16] R. Verger, "Interfacial activation" of lipases: facts and artifacts, Trends Biotechnol. 15 (1997) 32–38, https://doi.org/10.1016/S0167-7799(96)10064-0.
[17] J. Uppenberg, M.T. Hansen, S. Patkar, T.A. Jones, The sequence, crystal structure determination and refinement of two crystal forms of lipase B from *Candida antarctica*, Structure 2 (1994) 293–308, https://doi.org/10.1016/S0969-2126(00)00031-9.
[18] R.C. Rodrigues, J.J. Virgen-Ortíz, J.C.S. dos Santos, Á. Berenguer-Murcia, A.R. Alcantara, O. Barbosa, C. Ortiz, R. Fernandez-Lafuente, Immobilization of lipases on hydrophobic supports: immobilization mechanism, advantages, problems, and solutions, Biotechnol. Adv. 37 (2019) 746–770, https://doi.org/10.1016/j.biotechadv.2019.04.003.
[19] E.A. Manoel, J.C.S. dos Santos, D.M.G. Freire, N. Rueda, R. Fernandez-Lafuente, Immobilization of lipases on hydrophobic supports involves the open form of the enzyme, Enzym. Microb. Technol. 71 (2015) 53–57, https://doi.org/10.1016/j.enzmictec.2015.02.001.
[20] F. Rosenau, K. Jaeger, Bacterial lipases from *Pseudomonas*: regulation of gene expression and mechanisms of secretion, Biochimie 82 (2000) 1023–1032, https://doi.org/10.1016/S0300-9084(00)01182-2.
[21] S. Larson, J. Day, A. Greenwood, J. Oliver, D. Rubingh, A. McPherson, Preliminary investigation of crystals of the neutral lipase from *Pseudomonas fluorescens*, J. Mol. Biol. 222 (1991) 21–22, https://doi.org/10.1016/0022-2836(91)90732-L.
[22] N.S. Rios, B.B. Pinheiro, M.P. Pinheiro, R.M. Bezerra, J.C.S. dos Santos, L.R.B. Gonçalves, Biotechnological potential of lipases from *Pseudomonas*: sources , properties and applications, Process Biochem. 75 (2018) 99–120, https://doi.org/10.1016/j.procbio.2018.09.003.
[23] D.A. Sánchez, G.M. Tonetto, M.L. Ferreira, *Burkholderia cepacia* lipase: a versatile catalyst in synthesis reactions, Biotechnol. Bioeng. 115 (2018) 6–24, https://doi.org/10.1002/bit.26458.
[24] J. Gao, Y. Wang, Y. Du, L. Zhou, Y. He, L. Ma, L. Yin, W. Kong, Y. Jiang, Construction of biocatalytic colloidosome using lipase-containing dendritic mesoporous silica nanospheres for enhanced enzyme catalysis, Chem. Eng. J. 317 (2017) 175–186, https://doi.org/10.1016/j.cej.2017.02.012.
[25] H. Li, L. Ma, L. Zhou, J. Gao, Z. Huang, Y. He, Y. Jiang, Magnetic integrated metal/enzymatic nanoreactor for chemical warfare agent degradation, Colloids Surf. A Physicochem. Eng. Asp. 571 (2019) 94–100, https://doi.org/10.1016/j.colsurfa.2019.03.061.
[26] Y. Jiang, H. Liu, L. Wang, L. Zhou, Z. Huang, L. Ma, Y. He, L. Shi, J. Gao, Virus-like organosilica nanoparticles for lipase immobilization: characterization and

biocatalytic applications, Biochem. Eng. J. 144 (2019) 125–134, https://doi.org/10.1016/j.bej.2019.01.022.
[27] L. Zhou, J. Li, J. Gao, H. Liu, S. Xue, L. Ma, G. Cao, Z. Huang, Y. Jiang, Facile oriented immobilization and purification of his-tagged organophosphohydrolase on viruslike mesoporous silica nanoparticles for organophosphate bioremediation, ACS Sustain. Chem. Eng. 6 (2018) 13588–13598, https://doi.org/10.1021/acssuschemeng.8b04018.
[28] Y. Du, J. Gao, W. Kong, L. Zhou, L. Ma, Y. He, Z. Huang, Y. Jiang, Enzymatic synthesis of glycerol carbonate using a lipase immobilized on magnetic organosilica nanoflowers as a catalyst, ACS Omega 3 (2018) 6642–6650, https://doi.org/10.1021/acsomega.8b00746.
[29] K. Ashtari, K. Khajeh, J. Fasihi, P. Ashtari, A. Ramazani, H. Vali, Silica-encapsulated magnetic nanoparticles: enzyme immobilization and cytotoxic study, Int. J. Biol. Macromol. 50 (2012) 1063–1069, https://doi.org/10.1016/j.ijbiomac.2011.12.025.
[30] H. Vaghari, H. Jafarizadeh-Malmiri, M. Mohammadlou, A. Berenjian, N. Anarjan, N. Jafari, S. Nasiri, Application of magnetic nanoparticles in smart enzyme immobilization, Biotechnol. Lett. 38 (2015) 223–233, https://doi.org/10.1007/s10529-015-1977-z.
[31] K. Singh, A. Mishra, D. Sharma, K. Singh, Nanotechnology in enzyme immobilization: an overview on enzyme immobilization with nanoparticle matrix, Curr. Nanosci. 15 (2019) 234–241, https://doi.org/10.2174/1573413714666181008144144.
[32] M. Adeel, M. Bilal, T. Rasheed, A. Sharma, H.M.N. Iqbal, Graphene and graphene oxide: functionalization and nano-bio-catalytic system for enzyme immobilization and biotechnological perspective, Int. J. Biol. Macromol. 120 (2018) 1430–1440, https://doi.org/10.1016/j.ijbiomac.2018.09.144.
[33] S.S. Nadar, V.K. Rathod, Magnetic-metal organic framework (magnetic-MOF): a novel platform for enzyme immobilization and nanozyme applications, Int. J. Biol. Macromol. 120 (2018) 2293–2302, https://doi.org/10.1016/j.ijbiomac.2018.08.126.
[34] M. Bilal, Y. Zhao, T. Rasheed, H.M.N. Iqbal, Magnetic nanoparticles as versatile carriers for enzymes immobilization: a review, Int. J. Biol. Macromol. 120 (2018) 2530–2544, https://doi.org/10.1016/j.ijbiomac.2018.09.025.
[35] S.A. Ansari, Q. Husain, Potential applications of enzymes immobilized on/in nano materials: a review, Biotechnol. Adv. 30 (2012) 512–523, https://doi.org/10.1016/J.BIOTECHADV.2011.09.005.
[36] A. Arsalan, H. Younus, Enzymes and nanoparticles: modulation of enzymatic activity via nanoparticles, Int. J. Biol. Macromol. 118 (2018) 1833–1847, https://doi.org/10.1016/j.ijbiomac.2018.07.030.
[37] J. Kim, J.W. Grate, P. Wang, Nanobiocatalysis and its potential applications, Trends Biotechnol. 26 (2008) 639–646, https://doi.org/10.1016/j.tibtech.2008.07.009.
[38] E.P. Cipolatti, R.O. Henriques, D.E. Moritz, J.L. Ninow, D.M.G. Freire, E.A. Manoel, R. Fernandez-, Nanomaterials for biocatalyst immobilization – state of the art and future trends, RSC Adv.. 6 (2016) 104675–104692. doi:https://doi.org/10.1039/c6ra22047a.
[39] C. Garcia-Galan, Á. Berenguer-Murcia, R. Fernandez-Lafuente, R.C. Rodrigues, Potential of different enzyme immobilization strategies to improve enzyme performance, Adv. Synth. Catal. 353 (2011) 2885–2904, https://doi.org/10.1002/adsc.201100534.
[40] A. Miszczyk, K. Darowicki, Study of anticorrosion and microwave absorption properties of NiZn ferrite pigments, Microwaves (1) (2011) 13–21, https://doi.org/10.1108/00035591111097657.
[41] N.S. Rios, D.M.A. Neto, J.C.S. dos Santos, P.B.A. Fechine, R. Fernández-Lafuente, L.R.B. Gonçalves, Comparison of the immobilization of lipase from *Pseudomonas fluorescens* on divinylsulfone or *p*-benzoquinone activated support, Int. J. Biol. Macromol. 134 (2019) 936–945, https://doi.org/10.1016/j.ijbiomac.2019.05.106.
[42] J.J. Virgen-Ortíz, V.G. Tacias-Pascacio, D.B. Hirata, B. Torrestiana-Sanchez, A. Rosales-Quintero, R. Fernandez-Lafuente, Relevance of substrates and products on the desorption of lipases physically adsorbed on hydrophobic supports, Enzym. Microb. Technol. 96 (2017) 30–35, https://doi.org/10.1016/j.enzmictec.2016.09.010.
[43] D.B. Hirata, T.L. Albuquerque, N. Rueda, J.J. Virgen-Ortíz, V.G. Tacias-Pascacio, R. Fernandez-Lafuente, Evaluation of different immobilized lipases in transesterification reactions using tributyrin: advantages of the heterofunctional octyl agarose beads, J. Mol. Catal. B Enzym. 133 (2016) 117–123, https://doi.org/10.1016/j.molcatb.2016.08.008.
[44] N. Rueda, J.C.S. dos Santos, R. Torres, C. Ortiz, O. Barbosa, R. Fernandez-Lafuente, Improved performance of lipases immobilized on heterofunctional octyl-glyoxyl agarose beads, RSC Adv. 5 (2015) 11212–11222, https://doi.org/10.1039/C4RA13338B.
[45] D.B. Hirata, T.L. Albuquerque, N. Rueda, J.M. Sánchez-Montero, E. Garcia-Verdugo, R. Porcar, R. Fernandez-Lafuente, Advantages of heterofunctional octyl supports: production of 1,2-dibutyrin by specific and selective hydrolysis of tributyrin catalyzed by immobilized lipases, ChemistrySelect 1 (2016) 3259–3270, https://doi.org/10.1002/slct.201600274.
[46] N.S. Rios, C. Mendez-Sanchez, S. Arana-Peña, N. Rueda, C. Ortiz, L.R.B. Gonçalves, R. Fernandez-Lafuente, Immobilization of lipase from *Pseudomonas fluorescens* on glyoxyl-octyl-agarose beads: improved stability and reusability, Biochim. Biophys. Acta, Proteins Proteomics 1867 (2019) 741–747, https://doi.org/10.1016/j.bbapap.2019.06.005.
[47] T.L.d. Albuquerque, N. Rueda, J.C.S. dos Santos, O. Barbosa, C. Ortiz, B. Binay, E. Özdemir, L.R.B. Gonçalves, R. Fernandez-Lafuente, Easy stabilization of interfacially activated lipases using heterofunctional divinyl sulfone activated-octyl agarose beads. Modulation of the immobilized enzymes by altering their nanoenvironment, Process Biochem. 51 (2016) 865–874, https://doi.org/10.1016/j.procbio.2016.04.002.
[48] L. Fernandez-Lopez, S.G. Pedrero, N. Lopez-Carrobles, J.J. Virgen-Ortíz, B.C. Gorines, C. Otero, R. Fernandez-Lafuente, Physical crosslinking of lipase from *Rhizomucor miehei* immobilized on octyl agarose via coating with ionic polymers, Process Biochem. 54 (2016) 81–88, https://doi.org/10.1016/j.procbio.2016.12.018.
[49] L. Fernandez-Lopez, J.J. Virgen-Ortíz, S.G. Pedrero, N. Lopez-Carrobles, B.C. Gorines, C. Otero, R. Fernandez-Lafuente, Optimization of the coating of octyl-CALB with ionic polymers to improve stability and decrease enzyme leakage, Biocatal. Biotransformation. 36 (2017) 47–56, https://doi.org/10.1080/10242422.2016.1278212.
[50] H. Zaak, L. Fernandez-Lopez, C. Otero, M. Sassi, R. Fernandez-Lafuente, Improved stability of immobilized lipases via modification with polyethylenimine and glutaraldehyde, Enzym. Microb. Technol. 106 (2017) 67–74, https://doi.org/10.1016/j.enzmictec.2017.07.001.
[51] V.G. Tacias-Pascacio, C. Ortiz, N. Rueda, Á. Berenguer-Murcia, N. Acosta, I. Aranaz, C. Civera, R. Fernandez-Lafuente, A.R. Alcántara, Dextran aldehyde in biocatalysis: more than a mere immobilization system, Catalysts 9 (2019) 622, https://doi.org/10.3390/catal9070622.
[52] C. Pizarro, M.C. Brañes, A. Markovits, G. Fernández-Lorente, J.M. Guisán, R. Chamy, L. Wilson, Influence of different immobilization techniques for *Candida cylindracea* lipase on its stability and fish oil hydrolysis, J. Mol. Catal. B Enzym. 78 (2012) 111–118, https://doi.org/10.1016/j.molcatb.2012.03.012.
[53] G. Fernandez-Lorente, M. Filice, D. Lopez-Vela, C. Pizarro, L. Wilson, L. Betancor, Y. Avila, J.M. Guisan, Cross-linking of lipases adsorbed on hydrophobic supports: highly selective hydrolysis of fish oil catalyzed by RML, JAOCS J. Am. Oil Chem. Soc. 88 (2011) 801–807, https://doi.org/10.1007/s11746-010-1727-2.
[54] Y. Bi, M. Yu, H. Zhou, H. Zhou, P. Wei, Biosynthesis of oleyl oleate in solvent-free system by *Candida rugosa* lipase (CRL) immobilized in macroporous resin with cross-linking of aldehyde-dextran, J. Mol. Catal. B Enzym. 133 (2016) 1–5, https://doi.org/10.1016/j.molcatb.2016.05.002.
[55] A.H. Orrego, R. Ghobadi, S. Moreno-Perez, A.J. Mendoza, G. Fernandez-Lorente, J.M. Guisan, J. Rocha-Martin, Stabilization of immobilized lipases by intense intramolecular cross-linking of their surfaces by using aldehyde-dextran polymers, Int. J. Mol. Sci. 19 (2018) 553, https://doi.org/10.3390/ijms19020553.
[56] S.S. Wong, L.J.C. Wong, Chemical crosslinking and the stabilization of proteins and enzymes, Enzym. Microb. Technol. 14 (1992) 866–874, https://doi.org/10.1016/0141-0229(92)90049-T.
[57] N. Rueda, J.C.S. dos Santos, C. Ortiz, R. Torres, O. Barbosa, R.C. Rodrigues, Á. Berenguer-Murcia, R. Fernandez-Lafuente, Chemical modification in the design of immobilized enzyme biocatalysts: drawbacks and opportunities, Chem. Rec. 16 (2016) 1436–1455, https://doi.org/10.1002/tcr.201600007.
[58] R.C. Rodrigues, Á. Berenguer-Murcia, R. Fernandez-Lafuente, Á. Berenguer-Murcia, R. Fernandez-Lafuente, Coupling chemical modification and immobilization to improve the catalytic performance of enzymes, Adv. Synth. Catal. 353 (2011) 2216–2238, https://doi.org/10.1002/adsc.201100163.
[59] O. Barbosa, C. Ortiz, Á. Berenguer-Murcia, R. Torres, R.C. Rodrigues, R. Fernandez-Lafuente, Glutaraldehyde in bio-catalysts design: a useful crosslinker and a versatile tool in enzyme immobilization, RSC Adv. 4 (2014) 1583–1600, https://doi.org/10.1039/c3ra45991h.
[60] E.H. Siar, S. Arana-Peña, O. Barbosa, M.N. Zidoune, R. Fernandez-Lafuente, Solid phase chemical modification of agarose glyoxyl-ficin: improving activity and stability properties by amination and modification with glutaraldehyde, Process Biochem. 73 (2018) 109–116, https://doi.org/10.1016/j.procbio.2018.07.013.
[61] Y. Wine, N. Cohen-Hadar, A. Freeman, F. Frolow, Elucidation of the mechanism and end products of glutaraldehyde crosslinking reaction by X-ray structure analysis, Biotechnol. Bioeng. 98 (2007) 711–718, https://doi.org/10.1002/bit.21459.
[62] I. Migneault, C. Dartiguenave, M.J. Bertrand, K.C. Waldron, Glutaraldehyde: behavior in aqueous solution, reaction with proteins, and application to enzyme crosslinking, Biotechniques 37 (2004) 790–802, https://doi.org/10.2144/04375RV01.
[63] R. Fernandez-Lafuente, C.M. Rosell, V. Rodriguez, J.M. Guisan, Strategies for enzyme stabilization by intramolecular crosslinking with bifunctional reagents, Enzym. Microb. Technol. 17 (1995) 517–523, https://doi.org/10.1016/0141-0229(94)00090-E.
[64] R. Kowal, R.G. Parsons, Stabilization of proteins immobilized on Sepharose from leakage by glutaraldehyde crosslinking, Anal. Biochem. 102 (1980) 72–76, https://doi.org/10.1016/0003-2697(80)90319-X.
[65] P. Monsan, Optimization of glutaraldehyde activation of a support for enzyme immobilization, J. Mol. Catal. 3 (1978) 371–384, https://doi.org/10.1016/0304-5102(78)80026-1.
[66] N.S. Rios, M.P. Pinheiro, J.C.S. dos Santos, T. de S. Fonseca, L.D. Lima, M.C. de Mattos, D.M.G. Freire, I.J. da Silva, E. Rodríguez-Aguado, L.R.B. Gonçalves, Strategies of covalent immobilization of a recombinant *Candida antarctica* lipase B on pore-expanded SBA-15 and its application in the kinetic resolution of (*R,S*)-Phenylethyl acetate, J. Mol. Catal. B Enzym. 133 (2016) 246–258, https://doi.org/10.1016/j.molcatb.2016.08.009.
[67] J.C.S. Santos, N. Rueda, A. Sanchez, R. Villalonga, L.R.B. Gonçalves, R. Fernandez-Lafuente, Versatility of divinylsulfone supports permits the tuning of CALB properties during its immobilization, Process Biochem. 5 (2015) 35801–35810, https://doi.org/10.1039/C5RA03798K.
[68] B.B. Pinheiro, N.S. Rios, E. Rodríguez Aguado, R. Fernandez-Lafuente, T.M. Freire, P.B.A. Fechine, J.C.S. dos Santos, L.R.B. Gonçalves, Chitosan activated with divinyl sulfone: a new heterofunctional support for enzyme immobilization. Application in the immobilization of lipase B from *Candida antarctica*, Int. J. Biol. Macromol. 130 (2019) 798–809, https://doi.org/10.1016/j.ijbiomac.2019.02.145.

[69] K. Czyzewska, A. Trusek, Catalytic membrane with the recombinant catalase from psychrotolerant bacteria Serratia sp. in dairy applications, Desalin. Water Treat. 128 (2018) 253–258, https://doi.org/10.5004/dwt.2018.22869.

[70] J.C. Begara-Morales, F.J. López-Jaramillo, B. Sánchez-Calvo, A. Carreras, M. Ortega-Muñoz, F. Santoyo-González, F.J. Corpas, J.B. Barroso, Vinyl sulfone silica: application of an open preactivated support to the study of transnitrosylation of plant proteins by S-nitrosoglutathione, BMC Plant Biol. 13 (2013) 61, https://doi.org/10.1186/1471-2229-13-61.

[71] A.L. Medina-Castillo, J. Morales-Sanfrutos, A. Megia-Fernandez, J.F. Fernandez-Sanchez, F. Santoyo-Gonzalez, A. Fernandez-Gutierrez, Novel synthetic route for covalent coupling of biomolecules on super-paramagnetic hybrid nanoparticles, J. Polym. Sci. A Polym. Chem. 50 (2012) 3944–3953, https://doi.org/10.1002/pola.26203.

[72] P. Prikryl, J. Lenfeld, D. Horak, M. Ticha, Z. Kucerova, Magnetic bead cellulose as a suitable support for immobilization of α-chymotrypsin, Appl. Biochem. Biotechnol. 168 (2012) 295–305, https://doi.org/10.1007/s12010-012-9772-y.

[73] K. Labus, A. Turek, J. Liesiene, J. Bryjak, Efficient Agaricus bisporus tyrosinase immobilization on cellulose-based carriers, Biochem. Eng. J. 56 (2011) 232–240, https://doi.org/10.1016/j.bej.2011.07.003.

[74] M.M. Jaworska, J. Bryjak, J. Liesiene, A search of an optimal carrier for immobilization of chitin deacetylase, Cellulose 16 (2009) 261–270, https://doi.org/10.1007/s10570-008-9242-4.

[75] J.C.S. Santos, N. Rueda, O. Barbosa, J.F. Fernández-Sánchez, A.L. Medina-Castillo, T. Ramón-Márquez, M.C. Arias-Martos, M.C. Millán-Linares, J. Pedroche, M. del M. Yust, L.R.B. Gonçalves, R. Fernandez-Lafuente, Characterization of supports activated with divinyl sulfone as a tool to immobilize and stabilize enzymes via multipoint covalent attachment. Application to chymotrypsin, RSC Adv. 5 (2015) 20639–20649, https://doi.org/10.1039/C4RA16926C.

[76] P. Zucca, E. Sanjust, Inorganic materials as supports for covalent enzyme immobilization: methods and mechanisms, Molecules 19 (2014) 14139–14194, https://doi.org/10.3390/molecules190914139.

[77] Y. Liu, C. Guo, C.-Z. Liu, Novel magnetic cross-linked lipase aggregates for improving the resolution of (*R,S*)-2-octanol, Chirality 27 (2015) 199–204, https://doi.org/10.1002/chir.

[78] R.M. Freire, T.S. Ribeiro, I.F. Vasconcelos, J.C. Denardin, E.B. Barros, G. Mele, L. Carbone, S.E. Mazzetto, P.B.A. Fechine, $MZnFe_2O_4$ (M = Ni, Mn) cubic superparamagnetic nanoparticles obtained by hydrothermal synthesis, J. Nanopart. Res. 15 (2013) 1616, https://doi.org/10.1007/s11051-013-1616-3.

[79] R.M. Freire, P.G.C. Freitas, W.S. Galvao, L.S. Costa, T.S. Ribeiro, I.F. Vasconcelos, J.C. Denardin, R.C. de Oliveira, C.P. Sousa, P. de-Lima-Neto, A.N. Correia, P.B.A. Fechine, Nanocrystal growth, magnetic and electrochemical properties of NiZn ferrite, J. Alloys Compd. 738 (2018) 206–217, https://doi.org/10.1016/j.jallcom.2017.12.088.

[80] R.M. Blanco, P. Terreros, M. Fernández-Pérez, C. Otero, G. Díaz-González, Functionalization of mesoporous silica for lipase immobilization: characterization of the support and the catalysts, J. Mol. Catal. B Enzym. 30 (2004) 83–93, https://doi.org/10.1016/j.molcatb.2004.03.012.

[81] H.M. Rietveld, Line profiles of neutron powder-diffraction peaks for structure refinement, Acta Crystallogr. 22 (1967) 151–152.

[82] L. Bleicher, J.M. Sasaki, C.O. Paiva Santos, Development of a graphical interface for the Rietveld refinement program DBWS, J. Appl. Crystallogr. 33 (2000) 1189, https://doi.org/10.1107/S0021889800005410.

[83] A.L. Patterson, The scherrer formula for X-ray particle size determination, Phys. Rev. 56 (1939) 978–982, https://doi.org/10.1103/PhysRev.56.978.

[84] D. Lombardo, O. Guy, Effect of alcohols on the hydrolysis catalyzed by human, Biochem. Biophys. Acta. 657 (1981) 425–437, https://doi.org/10.1016/0005-2744(81)90328-4.

[85] M.M. Bradford, A rapid and sensitive method for the quantitation of microgram quantities of protein utilizing the principle of protein-dye binding, Anal. Biochem. 72 (1976) 248–254, https://doi.org/10.1016/0003-2697(76)90527-3.

[86] U.K. Laemmli, Cleavage of structural proteins during the assembly of the head of bacteriophage T4, Nature 227 (1970) 680–685, https://doi.org/10.1038/227680a0.

[87] C. Garcia-Galan, J.C.S. Dos Santos, O. Barbosa, R. Torres, E.B. Pereira, V.C. Corberan, L.R.B. Gonçalves, R. Fernandez-Lafuente, Tuning of Lecitase features via solid-phase chemical modification: effect of the immobilization protocol, Process Biochem.. 49 (2014) 604–616. doi:https://doi.org/10.1016/j.procbio.2014.01.028.

[88] J.P. Henley, A. Sadana, Categorization of enzyme deactivations using a series-type mechanism, Enzym. Microb. Technol. 7 (1985) 50–60, https://doi.org/10.1016/0141-0229(85)90013-4.

[89] N. Dogan, A. Bingolbali, L. Arda, D. Akcan, Synthesis, structure, and magnetic properties of Ni_{1-x} $Zn_xFe_2O_4$ nanoparticles, J. Supercond. Nov. Magn. 30 (2016) 3611–3617, https://doi.org/10.1007/s10948-016-3899-y.

[90] A.M. El-Sayed, Influence of zinc content on some properties of Ni-Zn ferrites, Ceram. Int. 28 (2002) 363–367, https://doi.org/10.1016/S0272-8842(01)00103-1.

[91] M. Abbas, B. Parvatheeswara Rao, C. Kim, Shape and size-controlled synthesis of Ni Zn ferrite nanoparticles by two different routes, Mater. Chem. Phys. 147 (2014) 443–451, https://doi.org/10.1016/j.matchemphys.2014.05.013.

[92] G. Kandasamy, D. Maity, Recent advances in superparamagnetic iron oxide nanoparticles (SPIONs) for in vitro and in vivo cancer nanotheranostics, Int. J. Pharm. 496 (2015) 191–218, https://doi.org/10.1016/j.ijpharm.2015.10.058.

[93] W.S. Galvão, D.M.A. Neto, R.M. Freire, P.B.A. Fechine, Super-paramagnetic nanoparticles with spinel structure: a review of synthesis and biomedical applications, Solid State Phenom. (2015)https://doi.org/10.4028/www.scientific.net/SSP.241.139.

[94] M. Virumbrales-del Olmo, A. Delgado-Cabello, A. Andrada-Chacón, J. Sánchez-Benítez, E. Urones-Garrote, V. Blanco-Gutiérrez, M.J. Torralvo, R. Sáez-Puche, Effect of composition and coating on the interparticle interactions and magnetic hardness of MFe_2O_4 (M = Fe, Co, Zn) nanoparticles, Phys. Chem. Chem. Phys. 19 (2017) 8363–8372, https://doi.org/10.1039/C6CP08743D.

[95] A.T. Raghavender, N. Biliškov, Ž. Skoko, XRD and IR analysis of nanocrystalline Ni-Zn ferrite synthesized by the sol-gel method, Mater. Lett. 65 (2011) 677–680, https://doi.org/10.1016/j.matlet.2010.11.071.

[96] P. Esmaeilnejad-Ahranjani, M. Kazemeini, G. Singh, A. Arpanaei, Amine-functionalized magnetic nanocomposite particles for efficient immobilization of lipase: effects of functional molecule size on properties of the immobilized lipase, RSC Adv. 5 (2015) 33313–33327, https://doi.org/10.1039/C5RA02471D.

[97] G.S. Kiran, A.N. Lipton, J. Kennedy, A.D.W. Dobson, J. Selvin, A halotolerant thermostable lipase from the marine bacterium *Oceanobacillus sp*. PUMB02 with an ability to disrupt bacterial biofilms, Bioengineered 5 (2014) 305–318, https://doi.org/10.4161/bioe.29898.

[98] S. Kanimozhi, K. Perinbam, Synthesis of amino-silane modified superparamagnetic Fe_3O_4 nanoparticles and its application in immobilization of lipase from *Pseudomonas fluorescens* Lp1, Mater. Res. Bull. 48 (2013) 1830–1836, https://doi.org/10.1016/j.materresbull.2013.01.024.

[99] R.M. Bezerra, D.M.A. Neto, W.S. Galvão, N.S. Rios, A.C.L.d.M. Carvalho, M.A. Correa, F. Bohn, R. Fernandez-Lafuente, P.B.A. Fechine, M.C. de Mattos, J.C.S. dos Santos, L.R.B. Gonçalves, Design of a lipase-nano particle biocatalysts and its use in the kinetic resolution of medicament precursors, Biochem. Eng. J. 125 (2017) 104–115, https://doi.org/10.1016/j.bej.2017.05.024.

[100] P. Vrutika, M. Datta, Lipase from solvent-tolerant *Pseudomonas sp*. DMVR46 strain adsorb on multiwalled carbon nanotubes: application for enzymatic biotransformation in organic solvents, Appl. Biochem. Biotechnol. 177 (2015) 1313–1326, https://doi.org/10.1007/s12010-015-1816-7.

[101] A. Barth, Infrared spectroscopy of proteins, Biochim. Biophys. Acta Bioenerg. 1767 (2007) 1073–1101, https://doi.org/10.1016/j.bbabio.2007.06.004.

[102] M.T. Moreira, Y. Moldes-diz, G. Feijoo, Formulation of laccase nanobiocatalysts based on ionic and covalent interactions for the enhanced oxidation of phenolic compounds, Appl. Sci. 7 (2017) 851, https://doi.org/10.3390/app7080851.

[103] J. Lin, Q. Wen, S. Chen, X. Le, X. Zhou, L. Huang, Synthesis of amine-functionalized Fe_3O_4@C nanoparticles for laccase immobilization, Int. J. Biol. Macromol. 96 (2017) 377–383, https://doi.org/10.1016/j.ijbiomac.2016.12.051.

[104] B.D. Cullity, C.D. Graham, Introduction to Magnetic Materials, second ed. John Wiley & Sons, New Jersey, 2009.

[105] Q. Jin, G. Jia, Y. Zhang, Q. Yang, C. Li, Hydrophobic surface induced activation of *Pseudomonas cepacia* lipase immobilized into mesoporous silica, Langmuir 27 (2011) 12016–12024, https://doi.org/10.1021/la202794t.

[106] A. Bastida, P. Sabuquillo, P. Armisen, R. Fernández-Lafuente, J. Huguet, J.M. Guisán, A single step purification, immobilization, and hyperactivation of lipases via interfacial adsorption on strongly hydrophobic supports, Biotechnol. Bioeng. 58 (1998) 486–493, https://doi.org/10.1002/(SICI)1097-0290(19980605)58:5<486::AID-BIT4>3.0.CO;2-9.

[107] R. Fernandez-Lafuente, P. Armisén, P. Sabuquillo, G. Fernández-Lorente, J. M. Guisán, Immobilization of lipases by selective adsorption on hydrophobic supports, Chem. Phys. Lipids 93 (1998) 185–197, https://doi.org/10.1016/S0009-3084(98)00042-5.

[108] S. Arana-Peña, Y. Lokha, R. Fernández-Lafuente, Immobilization of Eversa lipase on octyl agarose beads and preliminary characterization of stability and activity features, Catalysts 8 (2018) 511, https://doi.org/10.3390/catal8110511.

[109] S. Arana-Peña, Y. Lokha, R. Fernández-Lafuente, Immobilization on octyl-agarose beads and some catalytic features of commercial preparations of lipase A from *Candida antarctica* (Novocor ADL): comparison with immobilized lipase B from *Candida antarctica*, Biotechnol. Prog. 35 (2019), e2735. https://doi.org/10.1002/btpr.2735.

[110] G. Fernández-Lorente, J.M. Palomo, M. Fuentes, C. Mateo, J.M. Guisán, R. Fernández-Lafuente, Self-assembly of *Pseudomonas fluorescens* lipase into bimolecular aggregates dramatically affects functional properties, Biotechnol. Bioeng. 82 (2003) 232–237, https://doi.org/10.1002/bit.10560.

[111] J.M. Palomo, C. Ortiz, G. Fernández-Lorente, M. Fuentes, J.M. Guisán, R. Fernández-Lafuente, Lipase–lipase interactions as a new tool to immobilize and modulate the lipase properties, Enzym. Microb. Technol. 36 (2005) 447–454, https://doi.org/10.1016/j.enzmictec.2004.09.013.

[112] J.M. Palomo, C. Ortiz, M. Fuentes, G. Fernandez-Lorente, J.M. Guisan, R. Fernandez-Lafuente, Use of immobilized lipases for lipase purification via specific lipase-lipase interactions, J. Chromatogr. A 1038 (2004) 267–273, https://doi.org/10.1016/j.chroma.2004.03.058.

[113] J.M. Palomo, M. Fuentes, G. Fernández-Lorente, C. Mateo, J.M. Guisan, R. Fernández-Lafuente, General trend of lipase to self-assemble giving bimolecular aggregates greatly modifies the enzyme functionality, Biomacromolecules 4 (2003) 1–6, https://doi.org/10.1021/bm025729+.

[114] M. Galvis, O. Barbosa, R. Torres, C. Ortiz, R. Fernandez-Lafuente, Effect of solid-phase chemical modification on the features of the lipase from *Thermomyces lanuginosus*, Process Biochem. 47 (2012) 460–466, https://doi.org/10.1016/j.procbio.2011.12.001.

[115] F. López-Gallego, T. Montes, M. Fuentes, N. Alonso, V. Grazu, L. Betancor, J.M. Guisán, R. Fernández-Lafuente, Improved stabilization of chemically aminated enzymes via multipoint covalent attachment on glyoxyl supports, J. Biotechnol. 116 (2005) 1–10, https://doi.org/10.1016/j.jbiotec.2004.09.015.

[116] O. Barbosa, R. Torres, C. Ortiz, R. Fernandez-Lafuente, The slow-down of the CALB immobilization rate permits to control the inter and intra molecular modification produced by glutaraldehyde, Process Biochem. 47 (2012) 766–774, https://doi.org/10.1016/j.procbio.2012.02.009.

[117] F. López-Gallego, L. Betancor, C. Mateo, A. Hidalgo, N. Alonso-Morales, G. Dellamora-Ortiz, J.M. Guisán, R. Fernández-Lafuente, Enzyme stabilization by

glutaraldehyde crosslinking of adsorbed proteins on aminated supports, J. Biotechnol. 119 (2005) 70–75, https://doi.org/10.1016/j.jbiotec.2005.05.021.
[118] J. Brandt, L. Andersson, J. Porath, Covalent attachment of proteins to polysaccharide carriers by means of benzoquinone, Biochim. Biophys. Acta 386 (1975) 196–202, https://doi.org/10.1016/0005-2795(75)90259-7.
[119] S.F. Li, Y.H. Fan, J.F. Hu, Y.S. Huang, W.T. Wu, Immobilization of *Pseudomonas cepacia* lipase onto the electrospun PAN nanofibrous membranes for transesterification reaction, J. Mol. Catal. B Enzym. 73 (2011) 98–103, https://doi.org/10.1016/j.molcatb.2011.08.005.
[120] H. Zaak, L. Fernandez-Lopez, S. Velasco-Lozano, M.T. Alcaraz-Fructuoso, M. Sassi, F. Lopez-Gallego, R. Fernandez-Lafuente, Effect of high salt concentrations on the stability of immobilized lipases: dramatic deleterious effects of phosphate anions, Process Biochem. 62 (2017) 128–134, https://doi.org/10.1016/j.procbio.2017.07.018.
[121] A. Sanchez, J. Cruz, N. Rueda, J.C.S. Dos Santos, R. Torres, C. Ortiz, R. Villalonga, R. Fernandez-Lafuente, Inactivation of immobilized trypsin under dissimilar conditions produces trypsin molecules with different structures, RSC Adv. 6 (2016) 27329–27334, https://doi.org/10.1039/c6ra03627a.
[122] A. Salis, M.S. Bhattacharyya, M. Monduzzi, V. Solinas, Role of the support surface on the loading and the activity of *Pseudomonas fluorescens* lipase used for biodiesel synthesis, J. Mol. Catal. B Enzym. 57 (2009) 262–269, https://doi.org/10.1016/j.molcatb.2008.09.015.
[123] M. Aghababaie, M. Beheshti, A. Razmjou, A.K. Bordbar, Covalent immobilization of *Candida rugosa* lipase on a novel functionalized Fe_3O_4@SiO_2 dip-coated nanocomposite membrane, Food Bioprod. Process. 100 (2016) 351–360, https://doi.org/10.1016/j.fbp.2016.07.016.
[124] M. Hajar, F. Vahabzadeh, Biolubricant production from castor oil in a magnetically stabilized fluidized bed reactor using lipase immobilized on Fe_3O_4 nanoparticles, Ind. Crop. Prod. 94 (2016) 544–556, https://doi.org/10.1016/j.indcrop.2016.09.030.
[125] L. Shen, Z. Chen, Critical review of the impact of tortuosity on diffusion, Chem. Eng. Sci. 62 (2007) 3748–3755, https://doi.org/10.1016/j.ces.2007.03.041.